

# Experimental retinal detachment in the cone-dominant ground squirrel retina: Morphology and basic immunocytochemistry

KENNETH A. LINBERG,<sup>1</sup> TSUTOMU SAKAI,<sup>1,3</sup> GEOFFREY P. LEWIS,<sup>1</sup>  
AND STEVEN K. FISHER<sup>1,2</sup>

<sup>1</sup>Neuroscience Research Institute, University of California at Santa Barbara, Santa Barbara

<sup>2</sup>Department of Molecular, Cellular and Developmental Biology, University of California at Santa Barbara, Santa Barbara

<sup>3</sup>Department of Ophthalmology, Jikei University School of Medicine, Tokyo, Japan

(RECEIVED November 14, 2001; ACCEPTED August 12, 2002)

## Abstract

The cellular responses of the cone-dominant ground squirrel retina to retinal detachment were examined and compared to those in rod-dominant species. Retinal detachments were made in California ground squirrels. The retinas were prepared for light, electron, and confocal microscopy. Tissue sections were labeled with antibodies to cone opsins, rod opsin, glial fibrillary acidic protein (GFAP), vimentin, synaptophysin, cytochrome oxidase, and calbindin D 28K. Wax sections were probed with the MIB-1 antibody to detect proliferating cells. By 10 h postdetachment many photoreceptor cells in the ground squirrel already show structural signs of apoptosis. At 1 day many photoreceptors have collapsed inner segments (IS), yet others still have short stacks of outer segment discs. At 3 days there is a marked increase in the number of dying photoreceptors. Rod and medium-/long-wavelength opsins are redistributed in the cell membrane to their synaptic terminals. At 7 days photoreceptor cell death has slowed. Some regions of the outer nuclear layer (ONL) have few photoreceptor somata. IS remnants are rare on surviving photoreceptors. At 28 days these trends are even more dramatic. Retinal pigmented epithelium (RPE) cells do not expand into the subretinal space. The outer limiting membrane (OLM) appears flat and uninterrupted. Müller cells remain remarkably unreactive; they show essentially no proliferation, only negligible hypertrophy, and there is no increase in their expression of GFAP or vimentin. Horizontal cells show no dendritic sprouting in response to detachment. The speed and extent of photoreceptor degeneration in response to detachment is greater in ground squirrel than in cat retina—only a small number of rods and cones survive at 28 days of detachment. Moreover, the almost total lack of Müller cell and RPE reactivity in the ground squirrel retina is a significant difference from results in other species.

**Keywords:** Rods, Cones, Müller cells, Ultrastructure, Immunocytochemistry

## Introduction

Retinal detachment in humans can result from a range of causes and most are successfully repaired by modern surgical techniques (Aylward, 1996). However, if the macula is involved, even successful reattachment does not assure the return of normal vision. Although retinal detachment can occur in various forms (Bradbury & Landers, 2001), it involves the physical separation of the retina from the retinal pigmented epithelium (RPE). Detachment initiates a cascade of molecular and cellular events ranging from changes in early gene expression to changes in protein expression, outer segment (OS) degeneration, and eventual photoreceptor cell death. In the species used in previous experiments, prominent neuronal

remodeling and gliosis occur in the inner retina (for reviews, see Fisher & Anderson, 2001; Fisher et al., 2001).

Until we initiated this series of studies, all animal models of detachment were in species with rod-dominated retinas. Thus, cones, the receptors most critical to human vision, have received less than their fair share of study (for review, see Fisher et al., 2001). Antibodies against cone opsins have allowed us recently to study some effects of detachment on cones in the feline retina (Mervin et al., 1999; Lewis et al., 1999b; Linberg et al., 2001; Rex et al., 2002). However, unlike cones in the rod-free human fovea, cat cones exist among a photoreceptor population dominated by rods even in the cone-rich *area centralis* (Steinberg et al., 1973).

In hopes of finding another system that more closely models the situation in the human macula, we turned to the cone-dominant retina of the California ground squirrel, *Spermophilus beecheyi*. This species has long been used for studying cone-based vision (Jacobs et al., 1976; Long & Fisher, 1983; Linberg et al., 1996). Its

Address correspondence and reprint requests to: Steven K. Fisher, Neuroscience Research Institute, University of California at Santa Barbara, Santa Barbara, CA 93106-5060, USA. E-mail: fisher@lifesci.ucsb.edu

photoreceptor mosaic has been carefully mapped (Kryger et al., 1998) and, on average, rods comprise only 14% of the overall photoreceptor population, S-cones 6%, and M-cones the remaining 80% (Kryger et al., 1998). Whereas some of the morphological and biochemical responses of this species are similar to those seen in our models of detachment in rod-dominated species, many proved dramatically different.

Portions of this report have appeared in abstract form (Linberg et al., 1999, 2000).

## Materials and methods

### Experimental animals

California ground squirrels (*Spermophilus beecheyi*) were captured locally and housed in the Central Vivarium at the University of California at Santa Barbara (UCSB). Animals were cared for by the resident veterinarian and their experimental use was conducted in compliance with both the guidelines of the UCSB Animal Care Council and the *ARVO Statement for the Use of Animals in Ophthalmic and Vision Research*.

### Retinal detachments

Experimental retinal detachments were created as described previously (Lewis et al., 1999a). In brief, detachments were made in the right eyes of 23 adult ground squirrels. A small incision was made in the region of the pars plana. A solution of 0.25% sodium hyaluronate (Healon, Pharmacia, Piscataway, NJ) was then infused between the neural retina and the RPE via a glass micropipette. Using an overdose of sodium pentobarbital, animals were sacrificed at 10 h, or 1, 3, 7, and 28 days later.

### Tissue preparation

Most of each specimen was taken for laser scanning confocal microscopy. Tissue was fixed in 4% paraformaldehyde in 0.1 M sodium cacodylate buffer (pH 7.4) using a method modified from Hale and Matsumoto (1993), and kept in this fixative at 4°C until ready for sectioning. The strip prepared for light and electron microscopy was fixed briefly in this same paraformaldehyde solution and subsequently fixed overnight at 4°C in a mixture of 1% paraformaldehyde and 1% glutaraldehyde in 0.086 M phosphate buffer, postfixed in 2% osmium tetroxide in the same buffer for 2 h, then dehydrated in a graded ethanol series, transferred through propylene oxide, and finally embedded in Spurr's resin.

### Light microscopy (LM)

One-micrometer sections were stained with toluidine blue and/or saturated aqueous paraphenylenediamine, and photographed with an Olympus BX60 microscope.

### Electron microscopy (EM)

Tissue was thin sectioned using a Sorvall MT2B ultramicrotome. Sections were placed on copper grids and stained with aqueous uranyl acetate and Reynold's lead citrate before being examined and photographed by either a Philips CM10 or a JEOL JEM-1230 transmission electron microscope.

### Proliferation assay

To evaluate the extent of cellular proliferation in the retina, retina samples were fixed overnight in the 4% paraformaldehyde solution described above. The tissue was then dehydrated in increasing concentrations of ethanol and embedded in paraffin (paraplast X-tra, Fisher Scientific, Pittsburgh, PA). The tissue was sectioned at 4  $\mu$ m and placed on capillary gap slides (Fisher Scientific) at which time they were dewaxed in xylene, rehydrated in graded ethanol, and stained with the MIB-1 antibody (1:100; Immunotech, Westbrook, ME) to the Ki67 protein using an automated tissue stainer (Techmate 1000; Ventana Medical Systems, Tucson, AZ).

### Immunocytochemistry

Retinal samples, approximately 2-mm square, were embedded in 5% agarose in phosphate buffered saline (PBS) and sectioned on a Vibratome (Technical Products International, Polysciences, Warrington, PA). One-hundred-micron-thick radial sections were incubated in normal donkey serum (1:20 in PBS containing 0.5% BSA, 0.1% Triton X-100, and 0.1% sodium azide hereafter referred to as "PBTA") overnight at 4°C on a tissue rotator. The next day the blocking serum was removed and the primary antibodies in PBTA were added. Four sets of double-label combinations were used: anti-GFAP (1:500; DAKO, Carpinteria, CA) with anti-rod opsin rho4D2 (1:50; gift from Dr. R. Molday); anti-M/L cone opsin (1:2000; gift from Dr. J. Nathans) with anti-vimentin (1:500; DAKO); anti-calbindin D 28K (1:1000; Sigma Chemical Co., St. Louis, MO) with anti-S cone opsin (1:2000; gift from Dr. J. Nathans); anti-synaptophysin (1:100; DAKO) with anti-cytochrome oxidase (1:1000, Molecular Probes, Eugene, OR). After rotating overnight at 4°C, the sections were rinsed in PBTA and incubated in the appropriate secondary antibodies (donkey anti-rabbit and anti-mouse conjugated to Cy3 as well as donkey anti-rabbit, conjugated to Cy2 were used at 1:200; Jackson ImmunoResearch, West Grove, PA). The sections were then rinsed in PBTA, mounted in n-propyl gallate in glycerol, and viewed on a laser scanning confocal microscope (BioRad 1024). During generation of confocal images, the gain and black levels were held constant in order to allow intensity comparisons between experimental conditions for any given antibody.

### Tissue sampling

In the ground squirrel eye, the linear optic nerve head (ONH) subdivides the retina into unequal dorsal and ventral domains (Fig. 1A). About 2 mm beneath the ONH lies the elongated visual streak containing the highest photoreceptor and ganglion cell densities (Long & Fisher, 1983; Kryger et al., 1998). Detachments were made only in the ventral domain, usually detaching most of this region (Fig. 1A, hatched area). A central vertical strip of tissue (Figs. 1A & 1B) was excised and processed for LM and EM, while the rest of the detached region was used for immunofluorescence microscopy. The vertical strip was divided into four sampling regions: **a** (dorsal, superior retina), **b** (visual streak region), **c** (ventral midperiphery), and **d** (ventral far periphery). When this excised strip is turned on its side, the relationship of the retina, both detached and attached regions, to the back of the eye (RPE, choroid, sclera) can be seen (Fig. 1B). Region **c** contains the area of "highest" detachment, and both regions **b** and **d** include transitional zones between detached and attached retina.

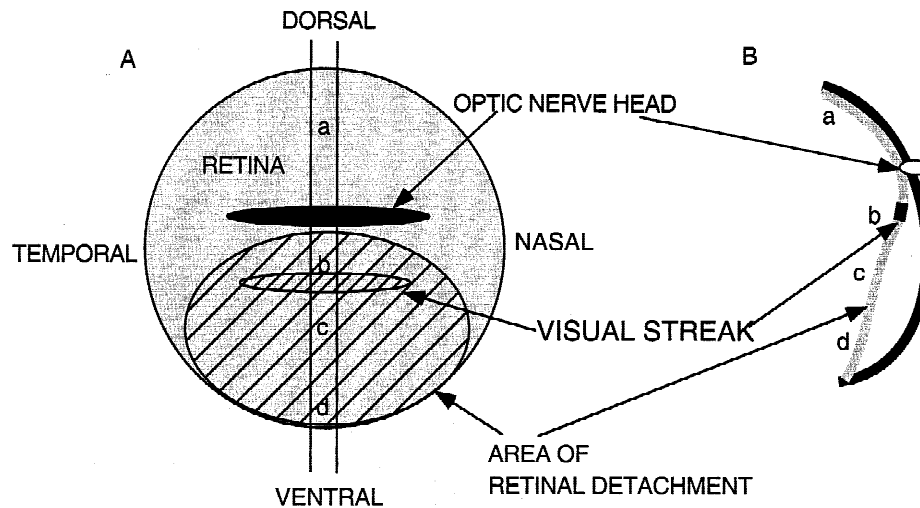


**Fig. 1.** (A) Diagram showing retinal landmarks and region of detachment. The elongated optic nerve head (ONH) subdivides the ground squirrel retina into dorsal and ventral domains. The visual streak, the region of highest photoreceptor and ganglion cell densities (Long & Fisher, 1983; Kryger et al., 1998) lies 2 mm ventral to the ONH. Detachments were made only in the ventral retina. Four broad regions of a vertical strip were routinely sampled: **a**: dorsal (superior) retina; **b**: visual streak region; **c**: ventral midperiphery; and **d**: ventral far periphery. (B) Diagram of the retinal regions studied. The excised strip described above, turned on its side, shows the relationship of retina (gray line), to the back of the eye (black line) consisting of the retinal pigmented epithelium, choroid, and sclera. Regions **b** and **d** contained transitional zones between detached and attached retina. Samples were routinely taken 1 mm from the superior and inferior edges (respectively) of each detachment. Sample area **c** contained the highest point of each detachment.

### Quantification

Manual counts of photoreceptors were made on single 1- $\mu$ m-thick resin sections from areas **b**, **c**, and **d** of normal and detached retinas. There were two animals per timepoint. The counts from each section were normalized to cells per millimeter of retina and then averaged for each detachment time (Fig. 2A). Counts of dying cells (Fig. 2B) in these toluidine blue-stained sections were based upon their distinctively dark, pyknotic appearance. These rounded profiles are easily distinguished from a population of elongate, darkly staining cells that normally are found in the retina of this species (Jacobs et al., 1976; see examples in Fig. 3C).

### Results

#### Morphology

##### Normal retina

Figs. 3A–3D depict sections of normal ground squirrel retina taken from sample areas **a–d**. Retinal thickness varies with retinal location in this species as was first shown by Long and Fisher (1983). The dorsal retina (area “**a**”) is relatively thin, with one to two rows of nuclei in the ONL (Fig. 3A). The portion of the retina containing the visual streak (region “**b**”) is the thickest with two to three rows of densely packed photoreceptors, a thick inner plexiform layer (IPL), several rows of ganglion cell perikarya (Fig. 3B), and a nerve fiber layer (NFL, not shown). The ventral midperiphery is of intermediate thickness (region “**c**”), with multiple rows of nuclei in both the ONL and ganglion cell layer (GCL) and a thick IPL (Fig. 3C). The population of rods increases ventrally from the visual streak (Kryger et al., 1998). They comprise only 4.6% of the population within the visual streak, 10–20% just ventral to it, and up to 32% in the inferior periphery (region “**d**”, Fig. 3D).

Differentiating rods from cones in ground squirrel retina is difficult in conventional histological preparations. In general, rods have slightly longer OS than cones and their IS lie slightly more vitread than those of cones (Fig. 3E). By EM in any given section, cone OS have many continuities between the OS discs and the plasma membrane (Fig. 3F), while in rod OS these are limited to the basal-most discs (Fig. 3J). Rod terminals are smaller than cone terminals and have fewer ribbons and synaptic invaginations (Fig. 3G). Rods and cones are, however, easily distinguished by labeling with antibodies to their specific opsins (rod opsin: Figs. 3H & 3I).

In this species, the apical processes of the RPE are very thick and contain large numbers of pigment granules. They drape the whole OS (Figs. 3A–3E) and form a particularly robust association with the photoreceptor layer.

##### Detached retina

**10 hours:** At 10 h, many photoreceptors are pyknotic and thus appear to be undergoing apoptosis (Figs. 4A & 4B). Some of these degenerate “in place,” with their cell body still connected to a recognizable synaptic terminal (Fig. 4G), as if the process occurs so rapidly that the cells do not have time to undergo the characteristic “rounding up.” Some photoreceptor nuclei are apparently extruded across the outer limiting membrane (OLM) into the subretinal space (SRS) (Fig. 4A). Based on their morphology, 5–6% of the photoreceptors are apoptotic at this time (Fig. 2B, Table 1).

Even at this early timepoint, the height of detachment is correlated with the severity of degeneration. In the center of the detachment (Fig. 4A), many IS and OS are degenerating. Gaps left by dying cells appear in the ONL; vacuolated cells and pyknotic nuclei are common in that layer. In a region of shallower detachment (Fig. 4B), many photoreceptors still retain their IS, some with recognizable OS (Fig. 4C). Near the transition zone to

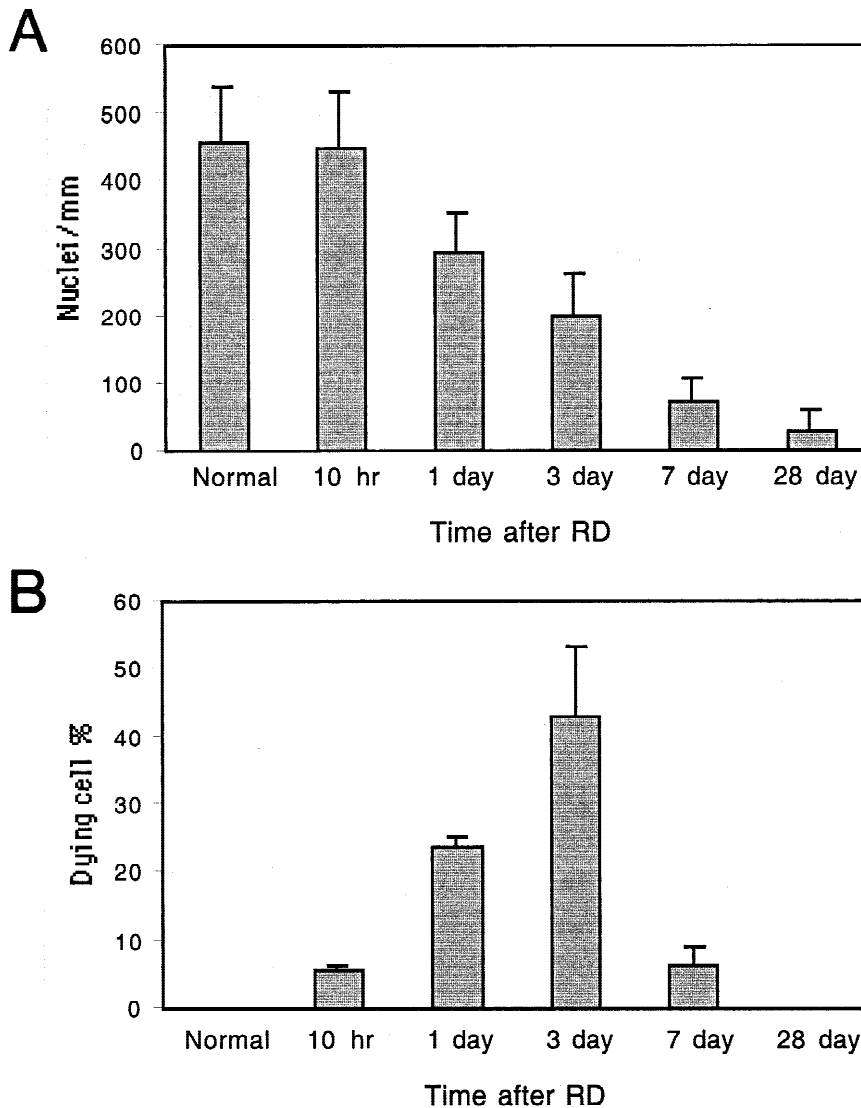


**Fig. 2.** (A) Graph showing the decrease in the average number of photoreceptor nuclei/mm with increasing detachment duration ( $n = 2$ ). Data are listed in Table 1A. (B) Graph depicting the average percentage of dying photoreceptors in the ONL at each time point ( $n = 2$ ). Data are listed in Table 1B. Error bars = 1 SD.

attached retina, the ONL is more uniform and shows even fewer signs of disruption (Fig. 4D) except for occasional large vacuoles among the synaptic terminals in the outer outer plexiform layer (OPL). In regions of higher detachment, OS discs often appear to fold over and fuse with the IS (Fig. 4F). This ectopic OS material can be observed in sections labeled with antibodies against rod opsin (Fig. 4E, arrows). Organelles with the appearance of lysosomes are more numerous in photoreceptor within detached regions (Figs. 4C & 4F) while organelles that appear to be autophagic bodies are more common in Müller cell cytoplasm (Fig. 4G).

*1 day:* Almost one out of four photoreceptors has the appearance of a dying cell (Table 1, Figs. 2B, 5A, 5B, 5D, & 5G), and as at 10 h, the severity of the effects reflects the height of detachment. Near the transition zone neither vacuoles nor pyknotic profiles are common (Fig. 5E). Surviving photoreceptors with intact IS have greatly truncated OS (Figs. 5A, 5B, & 5D) with their morphology ranging from quite normal (Fig. 5C) to highly disorganized (Figs. 5F & 5G). Ectopic whorls of OS membranes occur within the IS (Fig. 5H) as at 10 h (Fig. 4F).

After 1 day of detachment, the morphology of the RPE seems relatively unchanged although the apical process may be slightly

shortened (Figs. 5A & 5E). RPE cells still are seen engulfing OS debris (Fig. 5J), although most appears to be scavenged locally by macrophages in the SRS (see Figs. 6D, 7D, & 7H). There is no evidence of proliferation or the mounding and dedifferentiation of the apical RPE surface as is seen in detached cat (Anderson et al., 1983) and primate retina (Guérin et al., 1989).

*3 days:* Extensive cell death continues with, on average, 43% of the surviving photoreceptors in the ONL appearing apoptotic (Figs. 2B, 6A, 6B, & Table 1). The average density of photoreceptors in the ONL has dropped to 200/mm<sup>2</sup>, about 44% of normal (Fig. 2A, Table 1). However, even in the region with the highest detachment, the OPL neuropil appears relatively normal except for the presence of degenerating photoreceptor synaptic terminals (Fig. 6G). Although the outer surface of the retina in region c is flat and lacks normal IS, it is lined by wispy profiles of unknown cellular origin (Fig. 6A). There is no evidence of subretinal glial scars, proliferation in the inner retina, nor migration of inner retinal cells into the ONL. Macrophages are evident in the SRS (Fig. 6D). In peripheral, shallower regions, larger numbers of photoreceptors survive with short IS projecting into the SRS (Figs. 6B, 6D, & 6I). Near the edge of the detachment, aside from

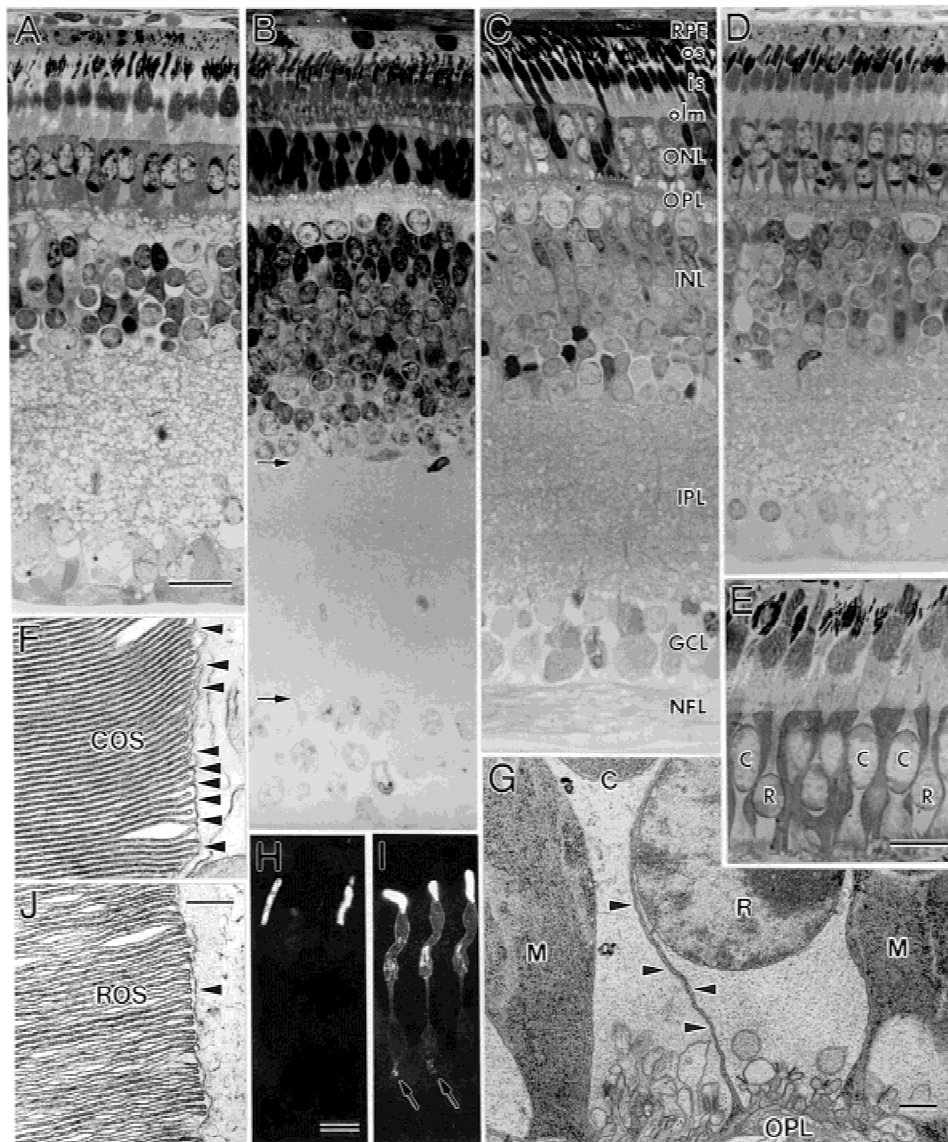


**Fig. 3.** Normal adult retina. Figs. 3A–3D are light micrographs (LMs) of the retinal regions **a–d** in Fig. 1, all at the same magnification (see scale bar in A). Note variations in retinal thickness with location. The various retinal layers are labeled in Fig. 3C. RPE: retinal pigmented epithelium; os: photoreceptor outer segments; is: photoreceptor inner segments; olm: outer limiting membrane; ONL: outer nuclear layer; OPL: outer plexiform layer; INL: inner nuclear layer; IPL: inner plexiform layer; GCL: ganglion cell layer; and NFL: nerve fiber layer. (A) Dorsal retina (region **a**, Figs. 1 & 2A). Photoreceptors in dorsal retina are thickset and populate an ONL only 1 or 2 rows thick. The GCL here is also relatively thin. Scale bar = 20  $\mu\text{m}$ . (B) Visual streak (region **b**, Figs. 1 & 2A). Photoreceptors are elongated; the ONL contains at least 2–3 rows of tightly packed perikarya. The GCL has 3–4 layers of nuclei underlain by a prominent NFL (not shown). The IPL (arrows) is thickest in this region. (C) Ventral midperiphery (region **c**, Figs. 1 & 2A). Intermediate in thickness between regions **a** and **b**, both the ONL and GCL of region **c** have several rows of nuclei; the nerve fiber layer (NFL) is distinctly thinner; the IPL only slightly so. Note that a subpopulation of photoreceptors has unusually dark cytoplasm. (D) Ventral periphery (region **d**, Figs. 1 & 2A). This region contains the lowest density of S-cones but the highest percentage of rods, up to 33% of all photoreceptors (Kryger et al., 1998). Although the retina is as thin as the dorsal retina, and the GCL is virtually a monolayer, the photoreceptors are thinner than those in the dorsal retina, and are more densely packed into the ONL. (E) LM of outer retina at higher magnification illustrates the relative morphology of rods (R) and cones (C) seen in region **d**. Note the longer OS of the rod, the vitread displacement of the rod ellipsoids, rod nuclei low in the ONL compared with those of cones, and the narrow rod terminals. Pigment granules crowd the RPE apical processes separating the photoreceptor OS. Scale bar = 10  $\mu\text{m}$ . (F) EM of the edges of a cone outer segment (COS). Note the numerous sites (arrowheads) where the cell's outer plasma membrane is continuous with its disc membranes. (See scale bar in J.) (G) EM of adjacent terminals of a cone (C) and a rod (R) separated by a thin rind of Müller cell cytoplasm (arrowheads). M: Müller cell outer limb. Scale bar = 1  $\mu\text{m}$ . (H) Confocal immunofluorescence image of rod OS labeled with the antibody to rod opsin with the gain set to allow visualization of just the OS. Scale bar = 10  $\mu\text{m}$ . (I) Confocal immunofluorescence image at an increased gain shows the faint outline of entire rods all the way to their terminals (arrows). Same magnification as H. (J) EM of the edge of a rod outer segment (ROS). ROS discs float free of any apparent connection to the cell's outer plasma membrane (arrowhead). Scale bar = 0.2  $\mu\text{m}$ .

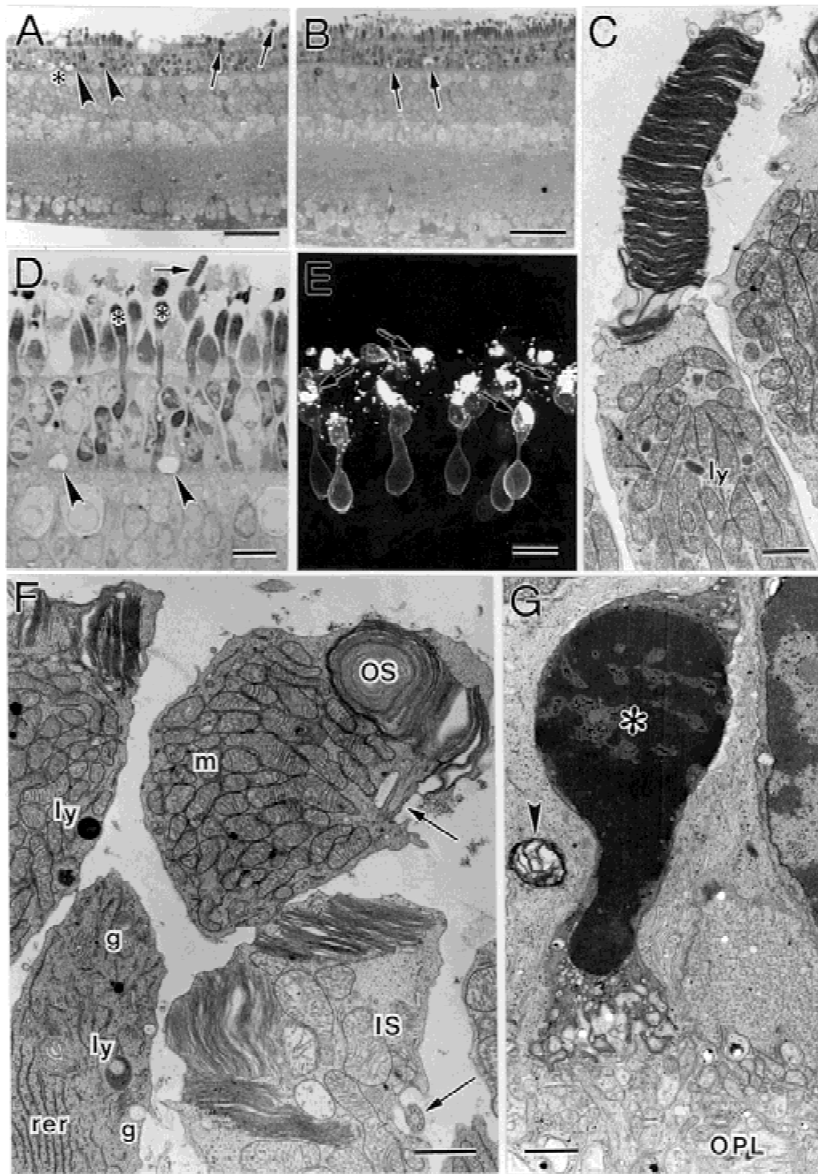


**Fig. 4.** 10-hour retinal detachment. (A) LM of retina from a severely affected region of the detachment where most photoreceptors lack both IS and OS. The density of photoreceptor nuclei in the ONL is uneven and this layer contains large vacuoles (\*) as well as apoptotic cells (arrowheads) some of which have been extruded (arrows) into the subretinal space (SRS). The inner retina appears normal. Scale bar = 50  $\mu\text{m}$ . (B) LM of a more intact region of retina where most photoreceptors retain IS projecting past the OLM. Although vacuoles are common in the ONL (arrows), apoptotic profiles are not. Scale bar = 50  $\mu\text{m}$ . (C) EM of relatively normal cone OS located in a shallow region of the detachment. Note the lysosomes (ly) in the IS. Scale bar = 1  $\mu\text{m}$ . (D) LM of outer retina from the inferior periphery. Photoreceptors are quite normal in appearance. No apoptotic photoreceptors are seen, though a few large vacuoles (arrowheads) border the OPL. Their IS have apically clumped mitochondria (\*), but only a few give rise to OS (arrow). Scale bar = 10  $\mu\text{m}$ . (E) Confocal immunofluorescence image of rods labeled with the antibody to rod opsin shows that many OS appear fused with their IS (arrows). Scale bar = 10  $\mu\text{m}$ . (F) EM of such fused OS and IS in the center of the detachment. Note connecting cilia (arrows) on two of these cells. *m*: ellipsoid mitochondria; *g*: Golgi complex; *ly*: lysosomes; and *rer*: rough endoplasmic reticulum. Scale bar = 1  $\mu\text{m}$ . (G) EM of receptor bases in the OPL. Some photoreceptors are undergoing apoptosis (\*). Its terminal is vesiculated compared with the terminal to the right. An autophagic vacuole (arrowhead) lies in the Müller cell cytoplasm. Scale bar = 1  $\mu\text{m}$ .

a few vacuoles near the OPL, the outer retina appears normal (Fig. 6E). Truncated OS (Fig. 6C; compare to 6F) or distorted OS (Fig. 6H) occur on some of the surviving photoreceptors.

RPE morphology continues to be relatively normal (Figs. 6A & 6E). At this timepoint we encountered a few examples of RPE cells spilling into the SRS (data not shown). Cellular debris in the SRS appears to preferentially associated with the RPE apical processes rather than the retinal surface (Fig. 6A).

**7 days:** Major thinning of the ONL is readily apparent in all regions of the detached tissue. Overall, photoreceptor density has been reduced to an average of 72 cells/ $\text{mm}^2$ , only 16% of normal, and at the height of the detachment, 33 cells/ $\text{mm}^2$  (Fig. 2A, Table 1). The number of apoptotic profiles has dropped dramatically averaging only 6% of the surviving cells (Fig. 2B, Table 1), although in the most severely affected central region, most of the few cells remaining in the ONL are pyknotic (Fig. 7E). In slightly less central regions, a few remaining cells elaborate IS (Figs. 7D & 7J) and even an occasional rudimentary OS (Figs. 7D & 7G). Few apoptotic profiles are seen at

such locations. In still more peripheral regions (Figs. 7A, 7B, & 7H), increasing numbers of surviving photoreceptors have IS, a significant number of which contain dark profiles (Figs. 7B & 7H) that by EM appear to be lysosomes (Fig. 7C). Only in the peripheral transition zone are photoreceptors found in greater numbers (Fig. 7F) and with a relatively normal morphology, except for the lack of OS.

The morphology of the RPE has not changed from that at the earlier timepoints (Figs. 7B, 7E).

**28 days:** At this time, the few surviving photoreceptors have a mushroom-like appearance (Fig. 10D, insets). Some of these still label with the antibody to rod opsin (Fig. 10D), further evidence that some rods remain. Surviving unlabeled photoreceptors are presumed to be cones.

The average density of photoreceptors in the 28-day detached retina has fallen to 28 cells/ $\text{mm}^2$ , only 6% of normal. At the height of the detachment there are only 3 cells/ $\text{mm}^2$ , and in the inferior periphery about 63/ $\text{mm}^2$  (Fig. 2A, Table 1). Few of the surviving photoreceptors appear pyknotic at this time (data not shown).

**Table 1.** Quantification of total photoreceptor nuclei/mm (A) and the percent of dying photoreceptors (B) in normal and detached ground squirrel retina<sup>a</sup>

Specimen	Area b	Area c	Area d	Average	Standard deviation
A. # Photoreceptor nuclei/mm					
Normal	500	510	363	457.7	82.1
10-h detachment	505 (101%)	485 (95%)	352 (97%)	447.3 (98%)	83.2
1-day detachment	363 (73%)	249 (49%)	274 (75%)	295.3 (65%)	59.9
3-day detachment	273 (55%)	155 (30%)	173 (48%)	200.3 (44%)	63.6
7-day detachment	87 (17%)	33 (6%)	97 (27%)	72.3 (16%)	34.4
28-day detachment	17 (3%)	3 (0.5%)	63 (17%)	27.7 (6%)	31.4
B. % dying Photoreceptors					
Normal	0	0	0	0	0
10-h detachment	5.2	6.3	4.8	5.4	0.8
1-day detachment	21.8	25.3	23.8	23.7	1.8
3-day detachment	43.0	53.2	33.1	43.1	10.0
7-day detachment	9.1	5.9	3.8	6.3	2.6
28-day detachment	0	0	0	0	0

<sup>a</sup>Regions **b**, **c**, and **d** correspond to retinal sample areas shown in Figs. 1A and 1B. Each time point represents the average of two animals.

In the center of the detachment there are long expanses of ONL largely lacking cell bodies, yet this layer remains discreet and recognizable, filled by the homogeneous and relatively featureless cytoplasm of Müller cell processes (Figs. 8A, 8B, & 9A). The occasional photoreceptor remains centrally though they lack most typical photoreceptor-like features (Fig. 8B, arrow). By EM these cells can be differentiated into probable rods (Fig. 9B) or cones (Fig. 9C) based on the structure of their synaptic terminals. A small number of cells in the ONL with a much lighter cytoplasm and lacking a synaptic zone (Fig. 8F) have the morphology of horizontal cells that appear to have migrated into this layer. One of these cells appears to be in transition between the inner nuclear layer (INL) and OPL in Fig. 8A. Photoreceptors are more numerous in more peripheral regions, and many of them have IS (Figs. 8D & 8E) a few of which give rise to a rudimentary OS (Figs. 8E & 8I). Even in the shallowest regions of the detachment (Fig. 8E), it is clear that the ONL has lost photoreceptors since they never comprise more than a single discontinuous row of cell bodies.

Interestingly, the OPL seems little affected by the loss of almost all photoreceptor synaptic terminals. By EM there is a recognizable zone near the border of the outer OPL that consists of clusters of fine processes (Figs. 8H, 8J, & 9A)—presumably residual groupings of processes that formed synapses with photoreceptors.

After a month of detachment, the RPE remains remarkably unchanged (Figs. 8A & 8B).

#### Müller cells

Despite the massive cell death in the ONL, it is the processes of Müller cells that keep that layer remarkably recognizable (Figs. 5B, 5D, 6A, 6B, 7D, & 7E). They also keep the OLM intact, forming a flat outer retinal surface. This is most obvious in regions where surviving photoreceptors are sparse or nonexistent (Figs. 5D, 5F, 6A, 7D, 7J, 8A, & 8B). The dark Müller cell cytoplasm around surviving photoreceptors contains numerous lysosomes and autophagic vacuoles (Figs. 5F, 5G, 6G, & 6I) as well as large numbers of 25–30 nm electron dense particles that are probably accumulations of glycogen granules and/or free ribosomes (Figs. 5I, 6J, 7I, 8C, 8G, & 8J). Both have been described in Müller cells of

the Korean ground squirrel (Rasmussen, 1974). An unusual occurrence in the OPL of detached retinas is the appearance of membrane-bound saccules that are outpouchings of Müller cell cytoplasm, crowded with free ribosomes (Fig. 5I). These usually occur in voids left by dying cells and often are several times larger than the example shown. Although Müller cells expand into the voids left as photoreceptors die, we saw no evidence of subretinal scar formation, hypertrophy within the retina, nor nuclear migration. Müller cell microvilli undergo changes in their morphology in the region of detachment—some elongate, some branch, and some form whorls or parallel membranous stacks (Figs. 6J, 7I, 8C, 8G, & 9A). Ribosomes do not occur normally in the microvilli, but extend into some of these apical formations (Figs. 6J, 8C, & 8G). At the latest stage of degeneration, the ONL is filled with whorls of Müller cell cytoplasm and membranes (Fig. 8J). In the longer term detachments, Müller cell columns across the inner retina become increasingly apparent (see Figs. 7E & 9A).

#### Proliferation

The use of the MIB-1 antibody to the Ki67 protein (Geller et al., 1995) on tissue sections from all timepoints as an assay for proliferation produced only a tiny number of labeled cells at the 10-h timepoint (0.92 cells/mm); no labeling was detectable at any other times.

#### Changes in Protein Expression

##### Visual proteins

As early as 10 h after detachment, the rod opsin antibody faintly stains the plasma membrane around rod cell bodies (Figs. 10A & 10B) as well as the OS. As OS shorten they also have an appearance of thickening, perhaps a correlate to the OS/IS fusion depicted in Fig. 4F. By 3 days postdetachment, OS degeneration has progressed as has the redistribution of rod opsin to the rod cell plasma membrane (Fig. 10C). It appears that staining in the IS has also increased. Any rods with OS at 28 days after detachment show

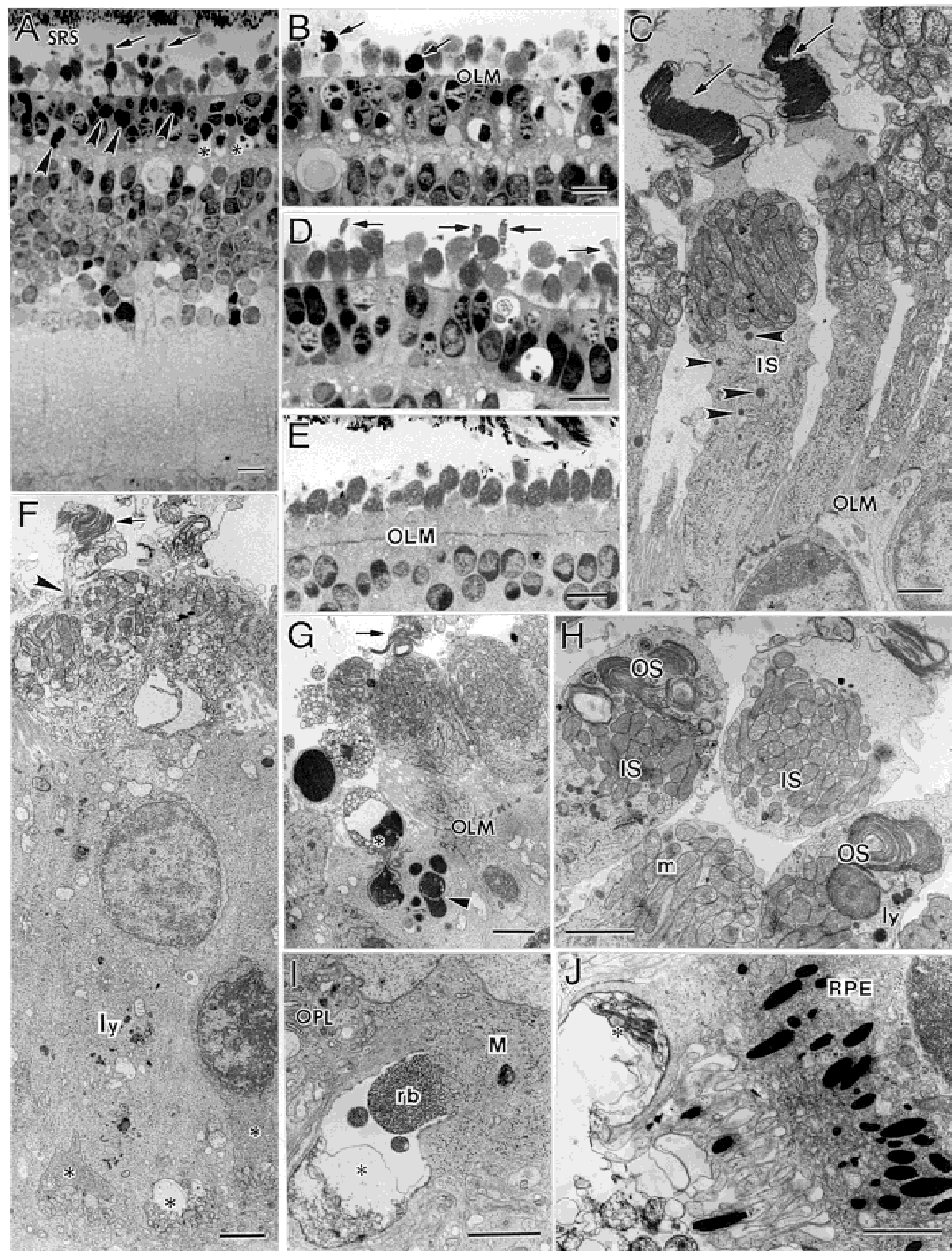


**Fig. 5.** 1-day retinal detachment. (A) LM of shallowly detached retina in region **b** near the visual streak. Although some OS remain (arrows), the IS and OS of most photoreceptors are disrupted. Apoptotic profiles (arrowheads) and vacuolized cells (\*) are common in the ONL. The inner retina seems unaffected. SRS: subretinal space. Scale bar = 10  $\mu\text{m}$ . (B) In region **b**, a deeper detachment than in part A. Some apoptotic photoreceptors (arrows) are extruded past the OLM into the SRS above the remaining photoreceptor IS. Scale bar = 10  $\mu\text{m}$ . (C) EM of photoreceptors from a shallow detachment in region **b**. Many of these cells have organized OS (arrows). The labeled IS contains several lysosomes (arrowheads). OLM: outer limiting membrane. Scale bar = 2  $\mu\text{m}$ . (D) In the ventral midperiphery (region **c**), the retina is widely separated from the RPE. As above, the ONL contains apoptotic photoreceptors and large vacuoles. Although some OS are visible (arrows) most remaining IS appear to be rounding-up. Scale bar = 10  $\mu\text{m}$ . (E) LM of the rod-rich ventral periphery (region **d**) near the transition zone between detached and attached retina. Though OS are mostly missing, the IS seem less disrupted and the ONL lacks apoptotic profiles or large vacuoles. OLM: outer limiting membrane. Scale bar = 10  $\mu\text{m}$ . (F) EM of the ONL in a region showing only two photoreceptors. Müller cell cytoplasm contains numerous lysosomes (ly) and apparently expands to occupy positions left by dying photoreceptors. A short OS stack (arrow) projects into the SRS from its connecting cilium (arrowhead). Three photoreceptor terminals (\*) lie at the bottom of the figure; the middle one shows signs of degeneration. Scale bar = 2  $\mu\text{m}$ . (G) EM of the outer detached retina from region **c**. One photoreceptor (\*) appears to be in the process of being extruded past the OLM into the SRS, while another cell apparently already was. A cluster of electron-dense bodies (arrowhead) may be nuclear fragments from yet another apoptotic cell. Arrow: OS. Scale bar = 2  $\mu\text{m}$ . (H) EM of fused IS and OS similar to those seen in Fig. 4F. m: ellipsoid mitochondria; and ly: lysosomes. Scale bar = 2  $\mu\text{m}$ . (I) EM of Müller cell cytoplasm (M) bordering the outer OPL. An outpocketing of cytoplasm crowded with granules presumed to be ribosomes (rb) projects into a void (\*) left by a degenerating photoreceptor terminal. These structures are quite common in detached retina but have not been described in normal retina. Scale bar = 2  $\mu\text{m}$ . (J) EM of the apical surface of the RPE showing that its apical processes are still ingesting OS debris: the remnants of a tip of a photoreceptor OS are being enveloped (\*). Scale bar = 2  $\mu\text{m}$ .

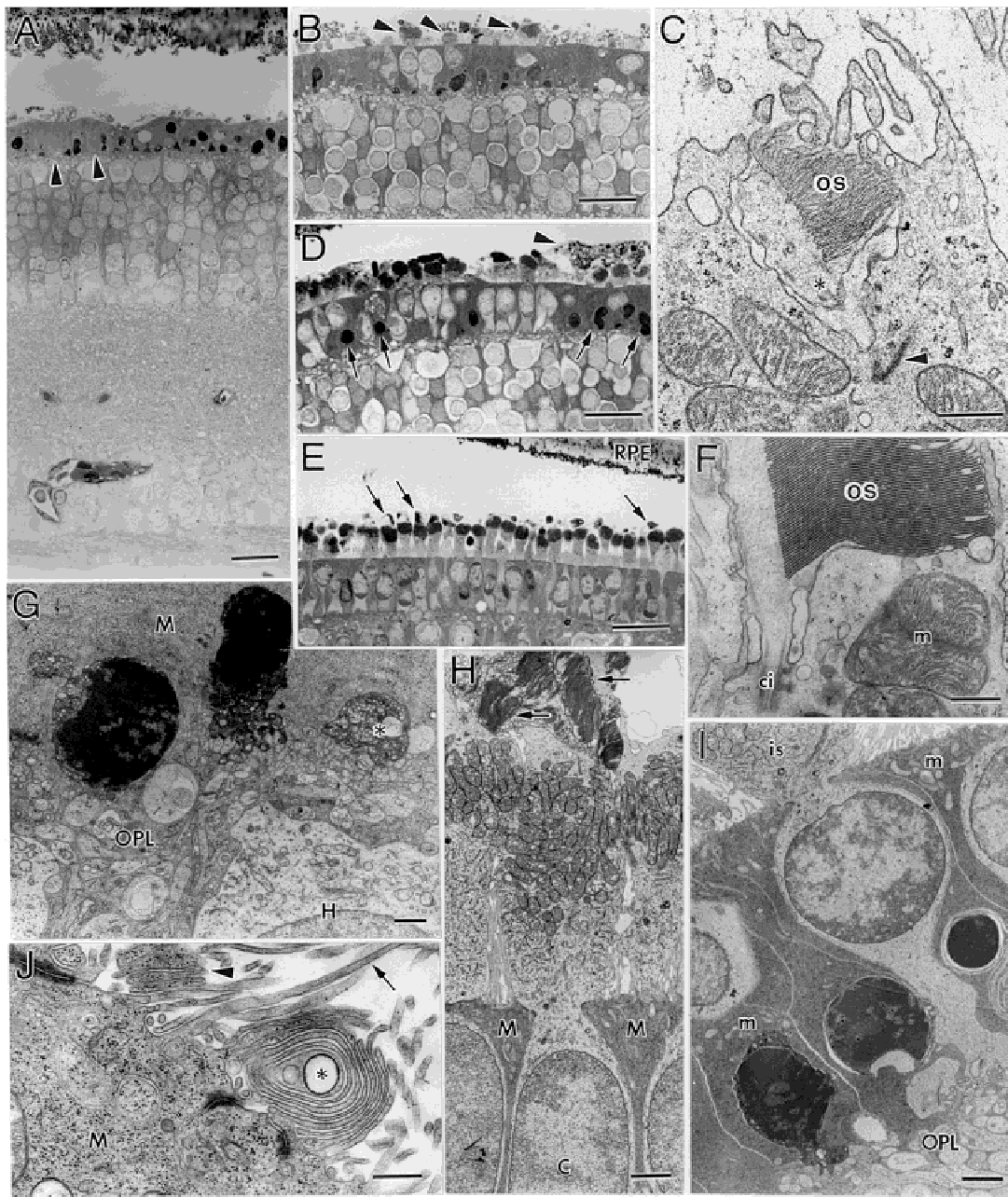


**Fig. 6.** 3-day retinal detachment. (A) LM of deeply detached retina from a region below the visual streak; the apparent proximity of RPE and retina seen here is an artifact of tissue processing and embedment. Most photoreceptors are gone while those remaining lack IS. Müller cell apical limbs appear to fill the space (arrowheads) left by the degenerating photoreceptors. The inner retina appears normal. Scale bar = 20  $\mu\text{m}$ . (B) The ONL in the mid-periphery is less degenerated than in part A with a number of intact photoreceptors among the numerous apoptotic cells. A few photoreceptors have IS (arrowheads). Scale bar = 20  $\mu\text{m}$ . (C) Even in regions of deepest detachments, a few surviving photoreceptors attempt to elaborate OS, a short stack whose ultrastructure is shown here. \*: connecting cilium seen in oblique section near the OS base; and arrowhead: edge of basal body associated with the connecting cilium. Scale bar = 0.5  $\mu\text{m}$ . (D) Another region of the ventral midperiphery showing a less disrupted ONL with 1–2 rows of photoreceptor nuclei, only a few of which (arrows) are apoptotic. Photoreceptor OS are absent or very degenerate. A large macrophage (arrowhead) appears to be scavenging photoreceptor debris. Scale bar = 20  $\mu\text{m}$ . (E) Transition zone in area **d** that shows little photoreceptor degeneration; the ONL contains 1–2 rows of oval nuclei. OS (arrows) crown many essentially normal photoreceptor IS. Note the dense apical clustering of pigment granules in the RPE. Scale bar = 20  $\mu\text{m}$ . (F) In the attached inferior periphery, the base of an intact cone OS appears ultrastructurally normal. m: ellipsoid mitochondria; and ci: connecting cilium. Scale bar = 0.5  $\mu\text{m}$ . (G) EM shows portions of three degenerating photoreceptors bordering the OPL. The apoptotic cell to the left is the most degenerated; the cell in the middle is still confluent with its degenerating terminal, while a heavily vacuolized terminal (\*) is the only visible part of the right hand cell. H: horizontal cell; and M: Müller cell apical limb. Scale bar = 1  $\mu\text{m}$ . (H) At the inferior periphery more cells survive the detachment, still elaborate OS packets (arrows), and have more normal-appearing IS. Note the electron-dense apical limbs of the Müller cells (M) separating the photoreceptors. C: cone cell body. Scale bar = 2  $\mu\text{m}$ . (I) The ONL of the inferior periphery is 1–2 cells thick. Here a surviving photoreceptor, lying among three apoptotic neighbors, is seen from its IS to its terminal in the OPL. Note how the mitochondria (m) appear pale inside the dark Müller cell cytoplasm. Scale bar = 2  $\mu\text{m}$ . (J) As shown by EM, the apical microvilli of ever increasing numbers of overlapping Müller cells (M) display changes from their normal morphology. Some elongate (arrow), others form stacks (arrowhead), or whorls (\*). Scale bar = 0.5  $\mu\text{m}$ .

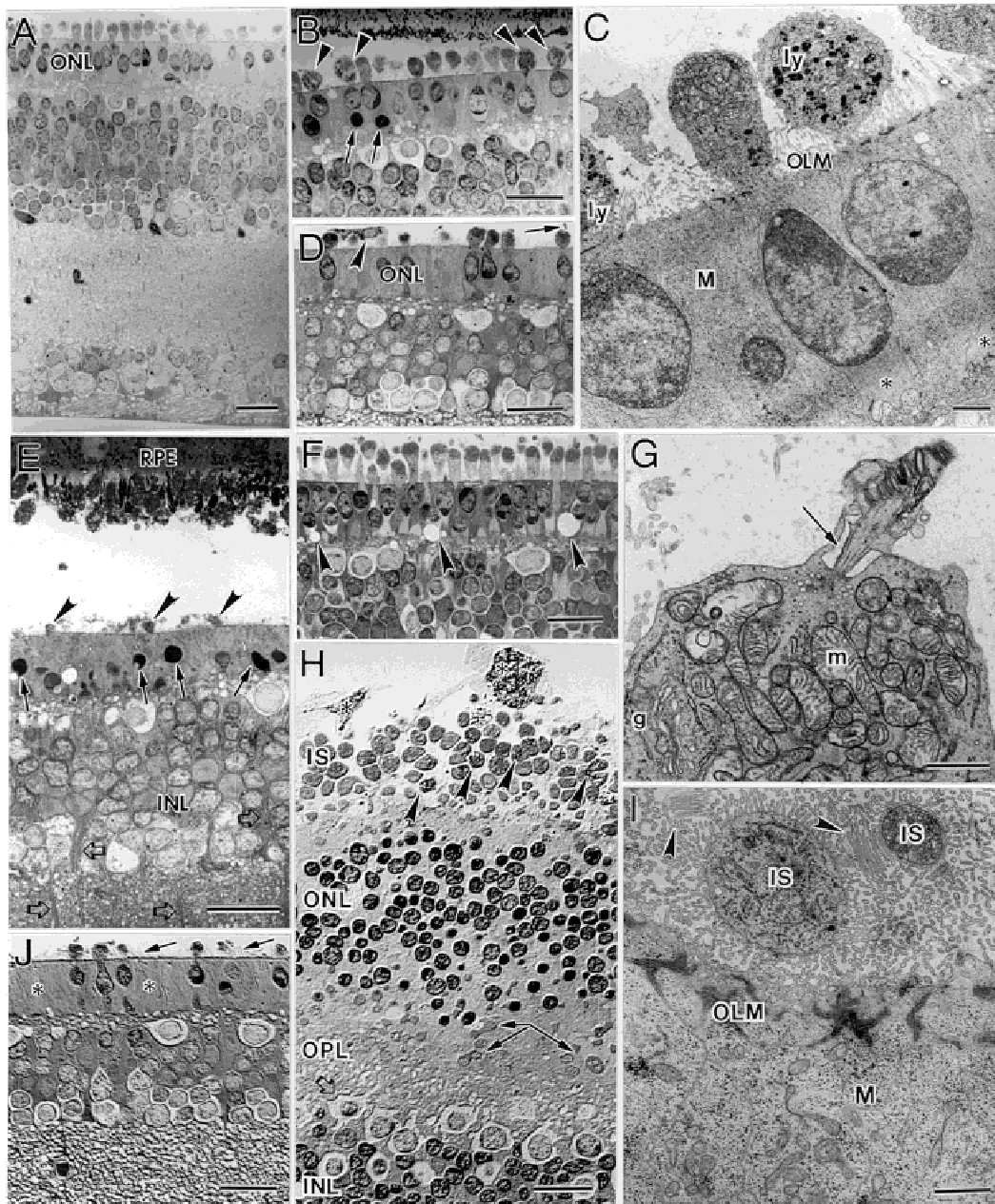


**Fig. 7.** 7-day retinal detachment. (A) LM of detached retina in region **b** near the visual streak. The ONL shows a range of degeneration from mild (on the left) to more severe (on the right) with many photoreceptors already lost. Scale bar = 20  $\mu\text{m}$ . (B) LM of outer retina in a region showing a greater degree of degeneration. IS, where present, appear short and rounded-up; some contain dark profiles (arrowheads). Apoptotic cells are seen in the ONL (arrows). Scale bar = 20  $\mu\text{m}$ . (C) In this same region of the ventral periphery, EM reveals that the “dark profiles” in the IS described in B appear to be large numbers of lysosomes (ly). These lysosomal profiles occur in a range of sizes and groupings. M: Müller cell cytoplasm; OLM: outer limiting membrane; and \* photoreceptor terminals. Scale bar = 2  $\mu\text{m}$ . (D) LM of a more central region of the detachment where few photoreceptors survive and patches of the ONL lack perikarya. A macrophage (arrowhead) lies in the SRS above the photoreceptor on the left while a short, rudimentary OS (arrow) projects apically from the photoreceptor at the right. Scale bar = 20  $\mu\text{m}$ . (E) Outer retina near the highest region of detachment in region **c**; the proximity of retina and RPE seen here is an artifact of fixation and embedment. The few remaining photoreceptor nuclei in the ONL are apoptotic (arrows). Only a few short and wispy IS (arrowheads) project beyond the OLM. Müller cell processes (open arrows) traverse the inner retina but do not extend beyond the OLM. INL: inner nuclear layer. Scale bar = 20  $\mu\text{m}$ . (F) Transition zone in region **d**. Aside from the loss of photoreceptor OS, few signs of photoreceptor degeneration are seen save for vacuoles (arrowheads) fronting on the OPL. Scale bar = 20  $\mu\text{m}$ . (G) EM of a rudimentary OS projecting into the SRS. It contains only short OS discs. m: ellipsoid mitochondria; g: Golgi complex; and arrow: connecting cilium. Scale bar = 1  $\mu\text{m}$ . (H) Oblique section through the outer retina as seen by LM using Nomarski optics. IS: inner segments; ONL: outer nuclear layer; OPL: outer plexiform layer; INL: inner nuclear layer; \*: macrophages; arrowheads: IS with dark profiles (lysosomes); thin arrows: photoreceptor terminals; and open arrow: horizontal cell showing three of its main dendritic trunks. Scale bar = 20  $\mu\text{m}$ . (I) EM shows that Müller cell apical microvilli crowd the SRS, closely encircling photoreceptor IS and forming stacked associations (arrowheads). OLM: outer limiting membrane. Scale bar = 1  $\mu\text{m}$ . (J) As seen by Nomarski optics, the ONL in region **b** near the visual streak has lost many photoreceptors. The remaining photoreceptor nuclei are unevenly scattered along the ONL; some regions lack nuclei altogether (\*). A thin fringe of Müller cell apical microvilli is visible just above the OLM (arrows). Scale bar = 20  $\mu\text{m}$ .

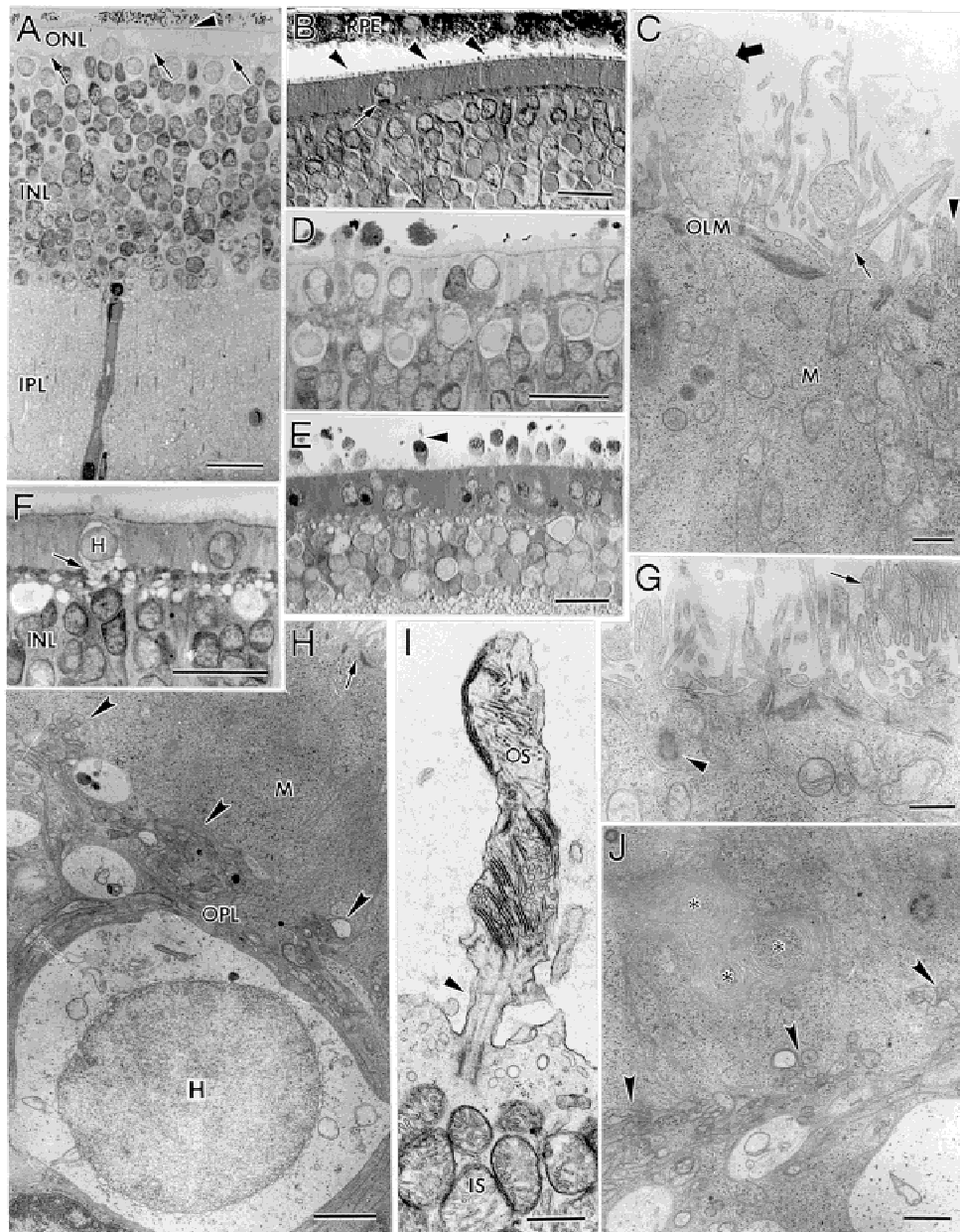


**Fig. 8.** 28-day retinal detachment. (A) LM of detached retina in region **b** near the visual streak. The ONL is devoid of photoreceptor nuclei and filled instead with Müller cell processes that maintain a flat retinal surface (arrowhead) at the OLM. Processes normally contacting photoreceptor synaptic terminals form a faint line (arrows) on the inner surface of the ONL; note the cell protruding through it. Both the thick INL and IPL appear normal. Scale bar = 20  $\mu\text{m}$ . (B) Nomarski LM of the outer retina in region **c**; its proximity to the RPE is an artifact of embedment. The cell body of a single photoreceptor, presumably a cone because of its broad synaptic zone (arrow), populates the ONL. No OS or IS are seen in the SRS; instead the retinal surface appears lined by a short fringe of clumped processes (arrowheads). Unlike conventional microscopy (compare to Figs. 8A & 8F), Nomarski optics reveal some columnar substructure to the overlapping Müller cell outer limbs in the ONL. Scale bar = 20  $\mu\text{m}$ . (C) EM reveals the substructure of those apical processes creating the short fringe distal to the OLM shown in part B. Müller cell apical microvilli form stacked associations (arrowhead), branch (arrow), and swell giving rise to growth cone-like structures (thick arrow). M: Müller cell cytoplasm. Scale bar = 0.5  $\mu\text{m}$ . (D) LM of the outer retina in a less severely afflicted central region. The ONL is comprised of a single, loosely packed row of photoreceptors, several of which have IS projecting into the SRS amid the fringe of processes described above. These IS retain their normal cytoplasmic polarity with their mitochondria amassed distally. Scale bar = 20  $\mu\text{m}$ . (E) LM of the outer retina in the inferior periphery where more photoreceptors survive. Many have IS; one sprouts a rudimentary OS apically (arrowhead). Scale bar = 20  $\mu\text{m}$ . (F) LM: in region **c**, a single photoreceptor lies to the right of a presumed horizontal cell (H) inverted into the ONL. Its basal cytoplasm (arrow) projects down into the OPL rather than terminating at a synaptic zone as with the photoreceptor shown in part B. INL: inner nuclear layer. Scale bar = 20  $\mu\text{m}$ . (G) EM of the fringe of apical Müller cell microvilli. Note the stacked association of modified microvilli (arrow) in the SRS. A centriole (arrowhead) lies in the apical Müller cell cytoplasm. Scale bar = 0.5  $\mu\text{m}$ . (H) Low power EM of the outer retina central to a detachment. Overlapping Müller cell processes fill the ONL from the OPL to the OLM (arrow). Clusters of processes line the inner ONL surface (arrowheads). The horizontal cell (H) has an electron lucent appearance compared to surrounding cells. Scale bar = 2  $\mu\text{m}$ . (I) In a region similar to that shown in part E and similar to another OS shown therein, EM shows a rudimentary OS projecting into the SRS. It contains loosely associated stacks of discs, and two sizes of tubules. Vesicles cluster in the apical IS cytoplasm near the base of the connecting cilium (arrowhead). Scale bar = 0.5  $\mu\text{m}$ . (J) EM reveals whorls of membranes (\*) resulting from the overlapping Müller cell apical processes. Clusters of processes (arrowheads) lie along the outer OPL. Scale bar = 1  $\mu\text{m}$ .

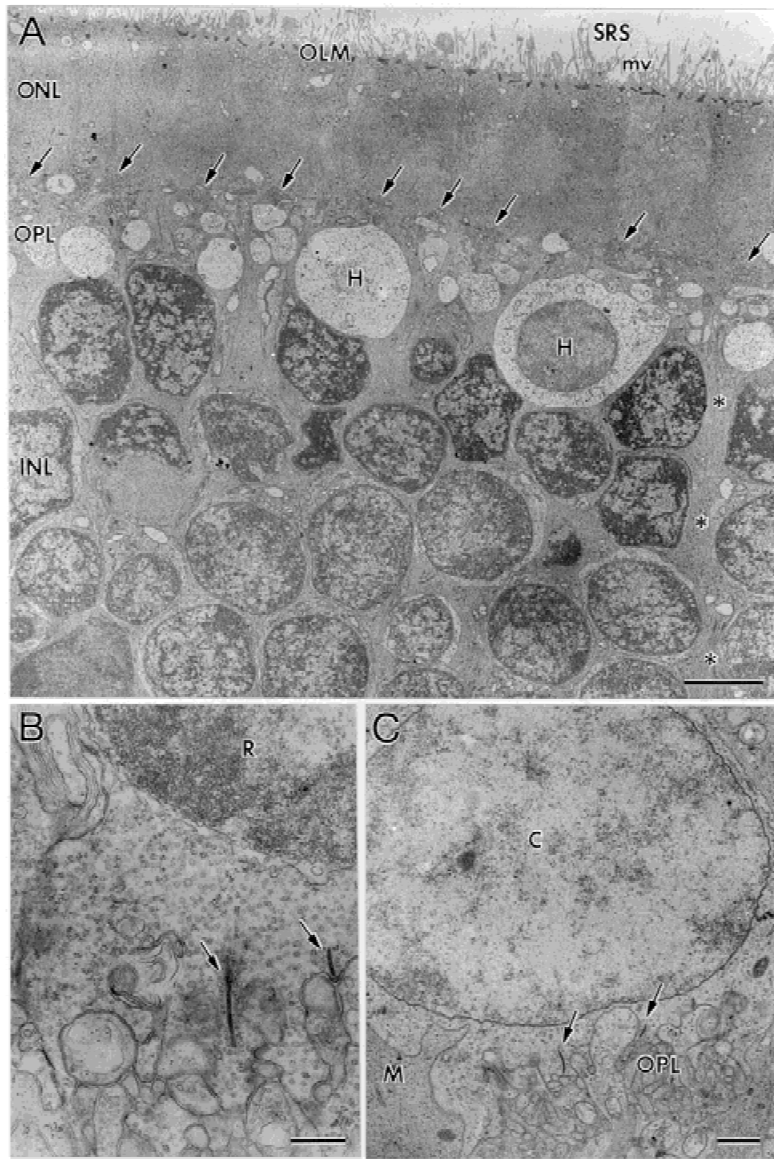


**Fig. 9.** 28-day retinal detachment. (A) Low-power EM showing a stretch of ONL lacking photoreceptor nuclei. Electron lucent processes and cell bodies of horizontal cells (H) are evident at the OPL which is lined apically by clusters of processes (arrows). A fringe of apical Müller cell microvilli (mv) distal to the OLM projects into the SRS. The inner retina (INL) appears undisturbed. \*: a vertical strip of Müller cell cytoplasm. Scale bar = 5  $\mu\text{m}$ . (B) EM of a rod-like terminal (R) surviving in region c. Arrows: synaptic ribbons. Scale bar = 0.5  $\mu\text{m}$ . (C) EM of a surviving cone-like terminal (C) in region c. OPL: outer plexiform layer; M: Müller cell cytoplasm; and arrows: synaptic ribbons. Scale bar = 0.5  $\mu\text{m}$ .

this same staining pattern although they have a vastly different shape than normal rods (Fig. 10D).

The antibody to S-cone opsin labels the OS of S-cones only, whereas the M/L-cone antibody used here labels the OS of both M- and S-cones in the ground squirrel (Figs. 10E & 10I; Kryger et al., 1998). At 10 h after detachment, we observe the same OS shortening in cones as in rods (Figs. 10F & 10J). By 3 days only short, stubby OS are labeled with the S-cone antibody (Fig. 10K). In contrast, antibodies to M/L-cone opsin show redistribution to the IS and plasma membrane in some cells, presumably the M-cones (Fig. 10G) since the labeling with the S-cone antibody never showed this phenomenon. By 28 days, only sparse and punctate labeling of rare cone OS occurred (Fig. 10H).

#### *Intermediate filament proteins*

The up-regulation of both glial fibrillary acidic protein (GFAP) and vimentin is an important hallmark of the Müller cell response to retinal detachment in rabbits (Francke et al., 2001), cats, and primates (Erickson et al., 1987; Guérin et al., 1990; Lewis et al., 1994, 1995).

In normal ground squirrel retina, antibodies to GFAP label only the astrocytes residing in the NFL (Figs. 10A–10D). There was essentially no increase in labeling of Müller cells with anti-GFAP at any detachment time.

The antibody to vimentin labels the cytoplasm of the entire Müller cell in normal ground squirrel retina (Fig. 10E). At 10 h after detachment, when photoreceptors are already dying, anti-vimentin labeling in the ONL appears to be intensifying (Fig. 10F) while labeling in the inner retina seems unchanged. This ONL labeling continues to increase slightly with increasing detachment time (Fig. 10G), and in the 28-day detachment demonstrates how completely the Müller cell cytoplasm dominates the ONL (Fig. 10H).

#### *Other proteins*

Anti-calbindin D 28K robustly stains horizontal cells in the normal squirrel retina as well as a population of bipolar cells (Fig. 10I), but does not label cones as it does in other species. These two cell types label with similar intensity in the 10-h detachment (Fig. 10J), but the labeling intensity in both decreases

in later detachments (Figs. 10K & 10L). We find no evidence of horizontal cell outgrowths beyond the OPL as has been seen in cat retina after detachment (Lewis et al., 1998).

The antibody against synaptophysin intensely labels all synaptic terminals in the OPL (Fig. 10M) and also labels the IS of some photoreceptors. After 10 h of detachment, the labeling of photoreceptor terminals is relatively unchanged (Fig. 10N), although labeling of shortened photoreceptor IS is greatly reduced. The alignment of photoreceptor terminals in the OPL remains similar to controls. By 3 days postdetachment, there are obvious gaps in the row of labeled terminals along the OPL (Fig. 10O), showing the effects of photoreceptor cell loss. Labeling increases in the cytoplasm of the remaining cell bodies and IS. By 28 days after detachment, anti-synaptophysin lightly labels the whole cell in the few surviving photoreceptors and the OPL is essentially unlabeled (Fig. 10P). The IPL is consistently labeled in all cases (Fig. 10P).

In normal retina, anti-cytochrome oxidase labels the apical mitochondrial mass in all photoreceptor IS (red label, Fig. 10M) and in the photoreceptor terminals (yellow, showing double-label with anti-synaptophysin). As expected, all retinal cells show some degree of positive labeling with this antibody (Fig. 10N). Labeling is reduced after detachment (Fig. 10O). More uniform labeling occurs in the Müller cell outer limbs that form the "ONL" at 28 days of detachment (Fig. 10P) when these processes are seldom interrupted by surviving photoreceptor perikarya.

## DISCUSSION

Here we establish the basic morphological responses of the ground squirrel retina to detachment. We chose to develop this system as a potential model for understanding the responses of human foveal cones to detachment. Although rods are 15 to 20 times more numerous than cones across most of the human retina (Curcio et al., 1990), they are absent from the fovea which when detached presents the most difficult challenges to visual recovery after reattachment surgery. If the ground squirrel retina is not a perfect model for the human fovea, it at least allows us to study the responses of cones when they are in the majority, something that does not occur even in the *area centralis* of the cat retina (Steinberg et al., 1973), nor the visual streak of the rabbit (Hughes, 1971). The fact that this system is also amenable to study by quantitative electroretinogram (ERG) analysis adds to its value (Jacobs et al., 2001). The results show that the ground squirrel photoreceptors undergo a rapid, severe degeneration resulting in the death of most of them, particularly in the zone of highest detachment. Interestingly, there was no detectable reaction on the part of inner retinal neurons except for the gradual loss of anti-calbindin D labeling in horizontal cells, nor any significant gliotic response on the part of Müller cells. Such rapidity and extent of photoreceptor loss after detachment has been documented only in one other species, the rabbit (Berglin et al., 1997; Faude et al., 2002). In rabbits as in cats, however, Müller cells mount a robust response to detachment that includes proliferation, hypertrophy, growth on the retinal surfaces, migration, and immunological up-regulation in their expression of intermediate filament proteins (Anderson et al., 1983; Erickson et al., 1983; Lewis et al., 1989; Fisher et al., 1991; Geller et al., 1995; Fisher & Anderson, 2001). Some of these events have been documented in monkey and human detachments (Guérin et al., 1990; Sethi et al., 2001), although data from primate fovea are sparse and human fovea nonexistent.

As in other species, the first morphological response occurs in the photoreceptor OS and IS with significant degeneration already in the 10-h detachments. Few OS are intact, most are significantly disrupted, and often short stacks of discs appear *within* the IS. Based on the immunolabeling with anti-rod opsin, these membranes are clearly of OS origin. These "ectopic" discs persist at 1 and 3 days postdetachment but are rarely seen at 7 or 28 days since few IS remain centrally. At 10 h there is already rod opsin redistribution to the rod plasma membrane, a phenomenon seen in surviving rods all the way to 28-days postdetachment. While the latter is a common feature of detachment in other species, and of other photoreceptor degenerative diseases (Lewis et al., 1991; Fariss et al., 1997), the rapidity with which it occurs in the ground squirrel is unusual.

Another striking feature of the model is the rapidity with which photoreceptors die. Nearly 50% of the photoreceptor population is lost by 3 days and by 7 days few photoreceptors survive centrally (Table 1). By comparison, at least 50% of the photoreceptors are still present in the feline retina at 30 days of detachment (Erickson et al., 1983). Such extreme cell loss from the ONL does not occur, except in small patches, in the feline model. Berglin et al. (1997) showed, however, that detached rabbit retina can reach a state of almost total photoreceptor loss within a month or so. Rabbits and ground squirrels have little in common to suggest a mechanism for this phenomenon. The rabbit retina is rod dominated and has no intraretinal circulation (although supposedly this would have little effect on photoreceptors since it serves the inner retina almost exclusively). The ground squirrel is cone dominated and has prominent intraretinal blood vessels (see Figs. 3B, 6A, & 8A).

Apoptotic cells in the ground squirrel occur most frequently at 3 days, the same as observed in cat retina (Cook et al., 1995). The frequency with which dying cells are observed is reduced by 7 days postdetachment. Certainly this in part stems from the fact that so few cells are left to die. The observation, however, that only 6% of the few remaining cells appear apoptotic at this stage does suggest a real retardation of the rate of cell death. Indeed, apoptotic profiles are quite rare at 28 days even in peripheral regions of the detachment. If photoreceptor death is caused by hypoxia of the outer retina (see Mervin et al., 1999; Lewis et al., 1999b), then the decreasing amount of cell death could result from the greater availability of oxygen to surviving cells as many photoreceptors die off. This is consistent with evidence in this and other species that hyperoxia can rescue photoreceptors from the degeneration induced by detachment (Mervin et al., 1999; Sakai et al., 2001).

While the results presented here indicate that a small number of both rods and cones survive a month after detachment, it remains unclear whether one photoreceptor type survives better than the other when both are confronted by the same surgical insult. That cones greatly outnumber rods in squirrel retina suggests that the huge numbers of photoreceptors that die after detachment must predominantly be cones. Moreover, Sakai et al. (2001) postulate that rods in this species seemed intrinsically more resistant to the effects of detachment than cones based on immunocytochemical and TUNEL-labeling data. However, to date any actual loss of cones has been difficult to quantify because detachment seems to trigger the down-regulation of most of the proteins normally used as markers to identify them, most notably, of course, the cone opsins (Linberg et al., 2001; Rex et al., 2002). Indeed, calbindin D 28K which is a cone marker in many species does not stain ground squirrel cones at all. It is intriguing, however, to examine the photoreceptor counts presented in Table 1. When comparing sample areas **b** (regions near the visual streak averaging 5% rods) to

sample areas **d** (regions near the inferior periphery with up to 30% rods), it is interesting to note that the percent of surviving photoreceptors is not that much different between the two regions. This is not the result one might expect if one type of photoreceptor was dying preferentially, or if one type was causing the demise of the other as is the case in retinitis pigmentosa where rods afflicted with a genetic mutation eventually doom genetically normal cones causing the eventual loss of central vision (Carter-Dawson *et al.*, 1978; Farber *et al.*, 1994).

If the shear volume and rapidity of photoreceptor loss are striking features of the ground squirrel model, another is the lack of obvious Müller cell reactivity, a major difference from results of detachment in other species (see Fisher & Anderson, 2001; Fisher *et al.*, 2001). Müller cells show strong GFAP and vimentin up-regulation and hypertrophy in virtually all other species (Lewis *et al.*, 1995; Francke *et al.*, 2001), and a significant number of them proliferate. Evidence for these events was so rare in the ground squirrels that we conclude that they are not part of the repertoire

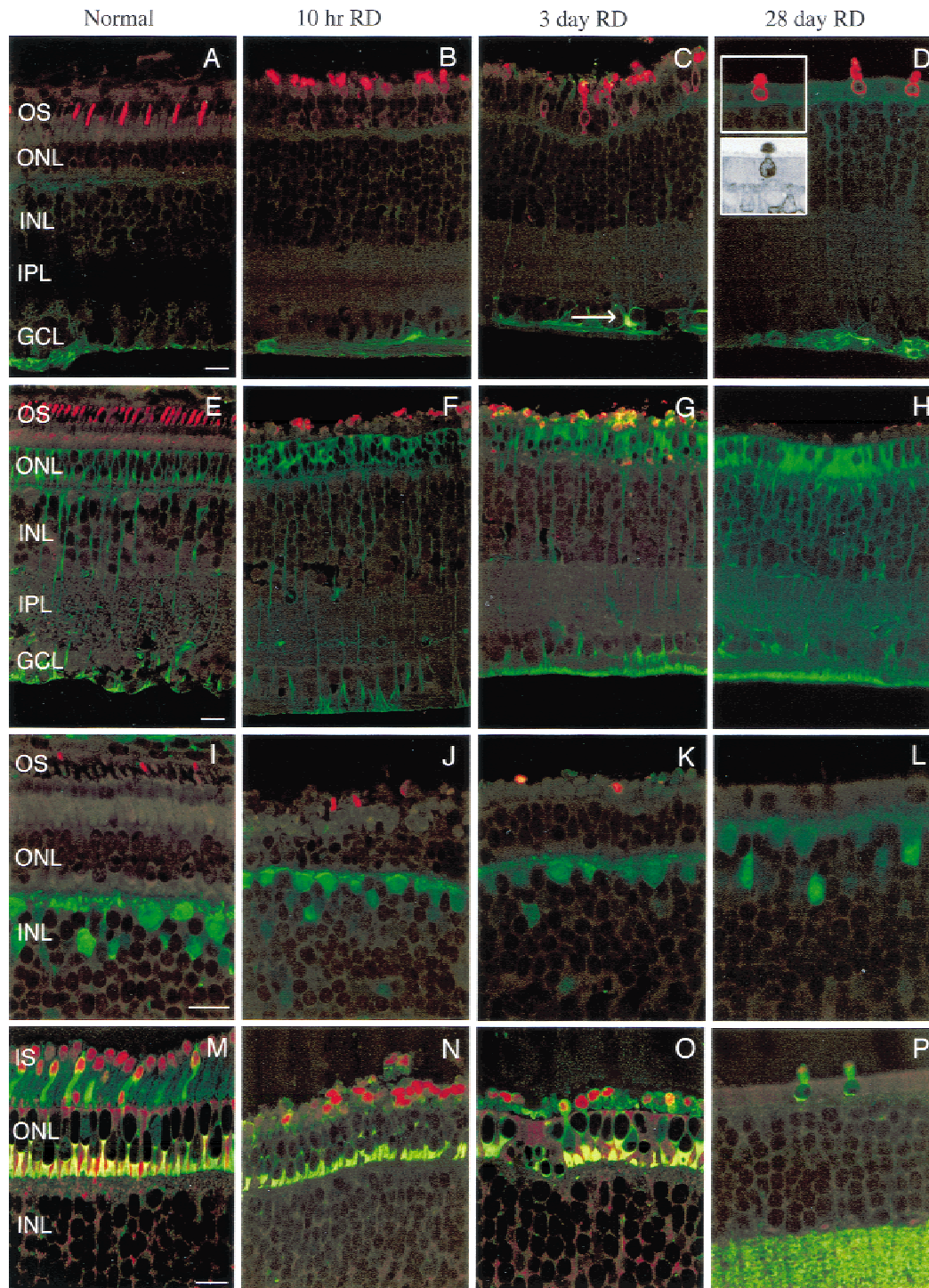


FIGURE 10

of Müller cell reactions in this species. If there is no Müller cell hypertrophy *per se*, the ground squirrel Müller cell population is still clearly reacting to the detachment in ways both obvious and subtle. As the photoreceptor population dwindles, Müller cells increasingly shoulder the responsibility of maintaining the OLM and appear to go to great lengths to maintain a flat and unbroken retinal surface as they expand into the voids left by the dying photoreceptors. This Müller cell response has been reported in other pathological conditions (Uga & Katsume, 1970). The lack of significant spaces in the ONL, even at the peak of photoreceptor loss, suggests that Müller cells respond quickly to the dying photoreceptors in a very specific manner. The presence of autophagic vacuoles and lysosomes in their cytoplasm after detachment suggests their role in the phagocytosis and lysis of photoreceptor debris. This is perhaps reflected by the apparent increase in the number of ribosomes in their cytoplasm with the extreme examples being the membrane-bound outpouchings of Müller cell cytoplasm filled with what appear to be free ribosomes. These structures are unknown in normal retina; they occur frequently in the early timepoints, but rarely so at 7 and 28 days. As the postdetachment interval increases, we also found larger and larger arrays of membranous whorls between the Müller cells filling the ONL. An additional morphological change in Müller cells is manifested at the OLM, where the apical fringe of uniform microvilli are replaced by elongate, enlarged, branched outgrowths. Thus, ground squirrel Müller cells are not unreactive, it is just that their reaction

is not characteristic of those observed in other, rod-dominated retinas, nor is it characteristic of the “gliotic” response of these cells in other retinal injuries. Indeed some reactions in the ground squirrel Müller cells are in the “opposite direction” to those in other species. Whereas Müller cells in the feline retina down-regulate, the amount of soluble molecules such as cellular retinaldehyde binding protein and glutamine synthetase in their cytoplasm after detachment, the ground squirrel cells appear to up-regulate these molecules (Sakai et al., 2001).

Curiously, the morphology of the ground squirrel RPE seems remarkably unchanged in response to detachment. While the apical processes seem foreshortened, they continue to project into the SRS and retain a population of resident pigment granules, maintaining the overall integrity and morphology of RPE monolayer.

### Conclusions

We chose to develop experimental detachment in this species as a potential model for understanding the fate of human foveal cones following macular detachment. The many differences we have identified between reactions in the ground squirrel and those in the rod-dominant retinas, as well as those in the few studies of macular cones that do exist (Guérin et al., 1989), raise the issue as to whether this is a good model for the fovea. Whether or not that is the case, it still provides us a system in which to study the reaction of cones and a system amenable to analysis by quantitative ERG (Jacobs et al., 2001). Furthermore, we can also perform retinal

---

**Fig. 10.** (*facing page*) Confocal immunofluorescence images of ground squirrel retina. (A–D) Sections labeled with antibodies to rod opsin (red) and GFAP (green). Scale bar = 10  $\mu\text{m}$ . (A) In normal retina rod opsin antibody labeling is restricted to the rod OS. Antibodies to GFAP label processes in the nerve fiber layer (NFL), proximal to the ganglion cell layer (GCL). (B) Similar staining patterns are seen in the 10-h detached retina, except that in addition to labeling the somewhat collapsed OS, anti-rod opsin faintly labels the rod cell plasma membrane around the cell body. (C) At 3 days after detachment, fewer intact OS are labeled with the antibody to rod opsin, but labeling has increased in the IS and the plasma membrane which in some cases stains all the way to the rod synaptic terminal. Labeling by anti-GFAP is still restricted to the NFL. Note the brightly labeled astrocyte cell body (arrow). (D) After 28 days of detachment, anti-rod opsin labels the few rods extant in the largely soma-free outer nuclear layer (ONL), but the once elongate cells are shrunken. Upper inset: The antibody against rod opsin labels a single rod that resembles the photoreceptor below. Lower inset: LM of an isolated surviving photoreceptor in the ONL after 28 days. (E–H) Sections labeled with antibodies to M/L cone opsin (red) and vimentin (green). Scale bar = 10  $\mu\text{m}$ . (E) In normal retina, the antibody to M/L-opsin brightly labels the S- and M-cone OS and faintly labels the myoid region of their IS. Labeling by anti-vimentin labels Müller cells from their end feet proximal to the GCL to the outer limiting membrane (OLM) distal to the ONL. (F) After 10 h of detachment, anti-M/L cone opsin stains the cone OS and IS, both of which appear disrupted. Labeling by anti-vimentin in the inner retina appears unchanged compared to controls, but labeling of the ONL has increased. (G) After 3 days of detachment when there are few remaining OS, anti-M/L cone opsin appears to redistribute to the plasma membrane. A few labeled cone terminals can be seen. Labeling by the antibody to vimentin has increased in the end feet and around surviving photoreceptors in the ONL. (H) After 28 days of detachment, labeling with the antibody against M/L cone opsin has all but disappeared. The intensity of anti-vimentin labeling of the Müller cell end feet remains elevated as is the prominent labeling of the ONL. (I–L) Sections labeled with antibodies to S-cone opsin (red) and calbindin D 28K (green). Scale bar = 10  $\mu\text{m}$ . (I) In normal retina, the antibody against S-cone opsin labels only the S-cone OS. The antibody against calbindin D labels horizontal cells and an unidentified subpopulation of bipolar cells. (J) After 10 h of detachment, the labeling patterns for both antibodies remain unchanged from the controls. (K) After 3 days of detachment, only occasional scattered short OS stacks label with the S-cone opsin antibody. The labeling of horizontal cells by anti-calbindin D has decreased in intensity. (L) By 28 days after detachment no S-cone opsin antibody staining was observed. Labeling of horizontal cells by anti-calbindin D is still fainter, while the bipolar cells’ labeling remains bright. (M–P) Sections labeled with antibodies to cytochrome oxidase (red) and synaptophysin (green). Scale bar = 10  $\mu\text{m}$ . (M) In normal retina the antibody to cytochrome oxidase heavily labels the distal mitochondrial mass in all photoreceptor IS and colocalizes (yellow) with anti-synaptophysin in the photoreceptor synaptic terminals. Also labeled are the Müller cell mitochondria in processes along the OLM, between the photoreceptor terminals, and in processes in the OPL and INL. In addition to the photoreceptor terminals, anti-synaptophysin lightly labels all photoreceptor IS and heavily labels an unidentified photoreceptor subtype. (N) At 10 h postdetachment, labeling patterns for both probes seems similar save for the obvious disruption of the OS and IS. (O) By 3 days after detachment labeling patterns for both antibodies remains the same, but the loss of many photoreceptors is evident. Faint, punctate anti-cytochrome oxidase labeling of Müller cell processes in the ONL is particularly noticeable in regions devoid of photoreceptor somata. (P) While the labeling pattern of the few remaining photoreceptors at 28 days after detachment is similar to earlier time points, save for a lack of photoreceptor terminals, anti-synaptophysin labeling of IPL processes is very bright while the labeling by anti-cytochrome oxidase of Müller cell processes in the ONL is faint and diffuse.

reattachments and study the cone regenerative process via both morphological and physiological methods. The lack of a "typical" Müller cell response may also prove useful in sorting out the relevance of gliosis to cellular damage during various retinal degenerations. Indeed, while we assume that Müller cells in the pure-cone primate fovea mount a gliotic response as found in the rod-dominated retina, this assumption has not, to our knowledge, been tested.

### Acknowledgments

The authors wish to thank Pharmacia, Inc. for providing the Healon and both Peter John Kappel and William P. Leitner for technical assistance. This research was supported by NIH grant EY00888.

### References

- ANDERSON, D.H., STERN, W.H., FISHER, S.K., ERICKSON, P.A. & BORGULA, G.A. (1983). Retinal detachment in the cat: The pigment epithelial-photoreceptor interface. *Investigative Ophthalmology and Visual Science* **24**, 906–926.
- AYLWARD, G.W. (1996). Latest developments in treating retinal detachment. *British Journal of Hospital Medicine* **55**, 100–103.
- BERGLIN, L., ALGVERE, P.V. & SEREGARD, S. (1997). Photoreceptor decay over time and apoptosis in experimental retinal detachment. *Graefe's Archive for Clinical and Experimental Ophthalmology* **235**, 306–312.
- BRADBURY, M.J. & LANDERS, M.B. III. (2001). Pathogenetic mechanisms of retinal detachment. In *Retina. III. Surgical Retina*, 3rd edition, ed. RYAN, S.J., pp. 1987–1993. St. Louis, Missouri: Mosby, Inc.
- CARTER-DAWSON, L.D., LAVAIL, M.M. & SIDMAN, R.L. (1978). Differential effect on the *rd* mutation on rods and cones in the mouse retina. *Investigative Ophthalmology and Visual Science* **7**, 489–498.
- COOK, B., LEWIS, G.P., FISHER, S.K. & ADLER, R. (1995). Apoptotic photoreceptor degeneration in experimental retinal detachment. *Investigative Ophthalmology and Visual Science* **36**, 990–996.
- CURCIO, C.A., SLOAN, K.R., KALINA, R.E. & HENDRICKSON, A.E. (1990). Human photoreceptor topography. *Journal of Comparative Neurology* **292**, 497–523.
- ERICKSON, P.A., FISHER, S.K., ANDERSON, D.H., STERN, W.H. & BORGULA, G.A. (1983). Retinal detachment in the cat: The outer nuclear and outer plexiform layers. *Investigative Ophthalmology and Visual Science* **24**, 927–942.
- ERICKSON, P.A., FISHER, S.K., GUÉRIN, C.J., ANDERSON, D.H. & KASKA, D.D. (1987). Glial fibrillary acidic protein increases in Müller cells after retinal detachment. *Experimental Eye Research* **44**, 37–48.
- FARBER, D.B., FLANNERY, J.G. & BOWES-RICKMAN, C. (1994). The *rd* mouse story: Seventy years of research on an animal model of inherited retinal degeneration. *Progress in Retinal and Eye Research* **13**, 31–64.
- FARISS, R.N., MOLDAV, R.S., FISHER, S.K. & MATSUMOTO, B. (1997). Evidence from normal and degenerating photoreceptors that two outer segment integral membrane proteins have separate transport pathways. *Journal of Comparative Neurology* **387**, 148–156.
- FAUDE, F., FRANCKE, M., MAKAROV, F., SCHUCK, J., GÄRTNER, U., REICHEL, W., WIEDEMANN, P., WOLBURG, H. & REICHENBACH, A. (2002). Experimental retinal detachment causes widespread and multi-layered degeneration in rabbit retina. *Journal of Neurocytology* **30**, 379–390.
- FISHER, S.K. & ANDERSON, D.H. (2001). Cellular effects of detachment on the neural retina and the retinal pigment epithelium. In *Retina. III. Surgical Retina*, 3rd edition, ed. RYAN, S.J., pp. 1961–1986. St. Louis, Missouri: Mosby, Inc.
- FISHER, S.K., ERICKSON, P.A., LEWIS, G.P. & ANDERSON, D.H. (1991). Intraretinal proliferation induced by retinal detachment. *Investigative Ophthalmology and Visual Science* **32**, 1739–1748.
- FISHER, S.K., STONE, J., REX, T.S., LINBERG, K.A. & LEWIS, G.P. (2001). Experimental retinal detachment: A paradigm for understanding the effects of induced photoreceptor degeneration. In *Concepts and Challenges in Retina Biology: A Tribute to John E. Dowling*, *Progress in Brain Research* **131**, ed. KOLB, H., RIPPES, H. & WU, S., 679–698, Elsevier, Amsterdam.
- FRANCKE, M., FAUDE, F., PANNICKE, T., BRINGMANN, A., ECKSTEIN, P., REICHEL, W., WIEDEMANN, P. & REICHENBACH, A. (2001). Electro-physiology of rabbit Müller cells in experimental retinal detachment and PVR. *Investigative Ophthalmology and Visual Science* **42**, 1072–1079.
- GELLER, S.F., LEWIS, G.P., ANDERSON, D.H. & FISHER, S.K. (1995). Use of the MIB-1 antibody for detecting proliferating cells in the retina. *Investigative Ophthalmology and Visual Science* **36**, 737–744.
- GUÉRIN, C.J., ANDERSON, D.H., FARISS, R.N. & FISHER, S.K. (1989). Retinal reattachment of the primate retina. Photoreceptor recovery after short-term detachment. *Investigative Ophthalmology and Visual Science* **30**, 1708–1725.
- GUÉRIN, C.J., ANDERSON, D.H. & FISHER, S.K. (1990). Changes in intermediate filament immunolabeling occur in response to retinal detachment and reattachment in primates. *Investigative Ophthalmology and Visual Science* **31**, 1474–1482.
- HALE, I.L. & MATSUMOTO, B. (1993). Resolution of subcellular detail in thick tissue sections: Immunohistochemical preparation and fluorescence confocal microscopy. In *Methods in Cell Biology: Cell Biological Applications of Confocal Microscopy*, ed. MATSUMOTO, B., pp. 289–324, Academic Press, San Diego, CA.
- HUGHES, A. (1971). Topographical relationships between the anatomy and physiology of the rabbit visual system. *Documenta Ophthalmologica* **30**, 33–159.
- JACOBS, G.H., FISHER, S.K., ANDERSON, D.H. & SILVERMAN, M.S. (1976). Scotopic and photopic vision in the California ground squirrel: Physiological and anatomical evidence. *Journal of Comparative Neurology* **165**, 209–227.
- JACOBS, G.H., CALDERONE, J.B., SAKAI, T., LEWIS, G.P. & FISHER, S.K. (2001). An animal model for studying cone function in retinal detachment. *Documenta Ophthalmologica* **104**, 119–132.
- KRYGER, Z., GALLI-RESTA, L., JACOBS, G.H. & REESE, B.E. (1998). The topography of rod and cone photoreceptors in the retina of the ground squirrel. *Visual Neuroscience* **15**, 685–691.
- LEWIS, G.P., ERICKSON, P.A., GUÉRIN, C.J., ANDERSON, D.H. & FISHER, S.K. (1989). Changes in the expression of specific Müller cell proteins during long-term retinal detachment. *Experimental Eye Research* **49**, 93–111.
- LEWIS, G.P., ERICKSON, P.A., ANDERSON, D.H. & FISHER, S.K. (1991). Opsin distribution and protein incorporation in photoreceptors after experimental retinal detachment. *Experimental Eye Research* **53**, 629–640.
- LEWIS, G.P., GUÉRIN, C.J., ANDERSON, D.H., MATSUMOTO, B. & FISHER, S.K. (1994). Experimental retinal detachment causes rapid changes in the expression of glial cell proteins. *American Journal of Ophthalmology* **118**, 368–376.
- LEWIS, G.P., MATSUMOTO, B. & FISHER, S.K. (1995). Changes in the organization and expression of cytoskeletal proteins during retinal degeneration induced by retinal detachment. *Investigative Ophthalmology and Visual Science* **36**, 2404–2416.
- LEWIS, G.P., LINBERG, K.A. & FISHER, S.K. (1998). Neurite outgrowth from bipolar and horizontal cells after experimental retinal detachment. *Investigative Ophthalmology and Visual Science* **39**, 424–434.
- LEWIS, G.P., LINBERG, K.A., GELLER, S.F., GUÉRIN, C.J. & FISHER, S.K. (1999a). Effects of the neurotrophin brain-derived neurotrophic factor in an experimental model of retinal detachment. *Investigative Ophthalmology and Visual Science* **40**, 1530–1544.
- LEWIS, G.P., MERVIN, K., VALTER, K., MASLIM, J., KAPPEL, P.J., STONE, J. & FISHER, S. (1999b). Limiting the proliferation and reactivity of retinal Müller cells during experimental retinal detachment: The value of oxygen supplementation. *American Journal of Ophthalmology* **128**, 165–172.
- LINBERG, K.A., SUEMUNE, S. & FISHER, S.K. (1996). Retinal neurons of the California ground squirrel, *Spermophilus beecheyi*: A Golgi study. *Journal of Comparative Neurology* **365**, 173–216.
- LINBERG, K.A., LEWIS, G.P., CHARTERIS, D.G. & FISHER, S.K. (1999). Experimental detachment in a cone dominant retina. *Investigative Ophthalmology and Visual Science* **40**, S951.
- LINBERG, K.A., LEWIS, G.P., SAKAI, T., LEITNER, W.P. & FISHER, S.K. (2000). A comparison of cellular responses to retinal detachment in cone- and rod-dominant species. *Investigative Ophthalmology and Visual Science* **41**, S570.
- LINBERG, K.A., LEWIS, G.P., SHAAW, C., REX, T.S. & FISHER, S.K. (2001). The distribution of S- and M-cones in normal and experimentally detached cat retina. *Journal of Comparative Neurology* **430**, 343–356.
- LONG, K.O. & FISHER, S.K. (1983). The distributions of photoreceptors and

- ganglion cells in the California ground squirrel, *Spermophilus beecheyi*. *Journal of Comparative Neurology* **221**, 329–340.
- MERVIN, K., VALTER K., MASLIM, J., LEWIS, G., FISHER, S. & STONE, J. (1999). Limiting photoreceptor death and deconstruction during experimental retinal detachment: The value of oxygen supplementation. *American Journal of Ophthalmology* **128**, 155–164.
- POLYAK, S.L. (1941). *The Retina*. Chicago, Illinois: University of Chicago Press.
- RASMUSSEN, K-E. (1974). The Müller cell: A comparative study of rod and cone retinas with and without retinal vessels. *Experimental Eye Research* **19**, 243–257.
- REX, T.S., FARISS, R.N., LEWIS, G.P., LINBERG, K.A., SOKAL, I. & FISHER, S.K. (2002). A survey of molecular expression by photoreceptors after experimental retinal detachment. *Investigative Ophthalmology and Visual Science* **43**, 1234–1247.
- SAKAI, T., LEWIS, G.P., LINBERG, K.A. & FISHER, S.K. (2001). The ability of hyperoxia to limit the effects of experimental detachment in cone-dominated retina. *Investigative Ophthalmology and Visual Science* **42**, 3264–3273.
- SETHI, C.S., LEWIS, G.P., LEITNER, W.P., MANN, D.L., CHARTERIS, D.G. & FISHER, S.K. (2001). Neuronal plasticity in complicated clinical and experimental retinal detachment. *Investigative Ophthalmology and Visual Science* **42**, S445.
- STEINBERG, R.H., REID, M. & LACY, P.L. (1973). The distribution of rods and cones in the retina of the cat (*Felis domesticus*). *Journal of Comparative Neurology* **148**, 229–248.
- UGA, S. & KATSUME, K. (1970). Electron microscopic observations on reactions of retinal Müller cells under pathological conditions. *Japanese Journal of Ophthalmology* **14**, 223–236.